aerospace

MDPI

Article

A Novel Decomposition Method for Manufacture Variations and the Sensitivity Analysis on Compressor Blades

Baojie Liu [1,2], Jiaxin Liu [2,3], Xianjun Yu [1,2,*] and Guangfeng An [1,2]

[1] Research Institute of Aero-Engine, Beihang University, Beijing 100083, China
[2] National Key Laboratory of Science & Technology on Aero-Engine Aero-Thermodynamics, Beihang University, Beijing 100083, China
[3] School of Energy and Power Engineering, Beihang University, Beijing 100083, China
* Correspondence: yuxj@buaa.edu.cn

Abstract: A high accuracy blade manufacture variation decomposition method was proposed to decompose the manufacture variations of compressor blades to systematic variation and non-systematic variation, which could help to clearly quantify the statistical characteristics of the effect of manufacture variations on the blade aerodynamic performance and to guide the modeling of manufacture variations in geometric uncertainty quantification and robust design studies. By conducting the decomposition of manufacture variations with 100 newly manufactured blades of a high-pressure compressor, it was found that the systematic variation could be modeled by using seven representative blade geometry design parameters well and the mean value of the non-systematic variation, which is determined by using the difference between the measured blade and systematically reconstructed blade, is close to zero. For the standard deviation of decomposed manufacture variations, the non-systematic variation accounts for about 40% of the whole, indicating that the systematic variation is the major component of the manufacture variation. However, based on statistical analysis and sensitivity analysis of the effects of the two types of manufacture variations on blade aerodynamic performance, it was found that the mean deviation of the blade loss mainly derives from systematic variations, and the loss dispersion caused by non-systematic variations is significantly greater than that caused by systematic variations. Furthermore, the blade loss at the high incidence angle is most sensitive to the inlet metal angle which belongs to the systematic variation. Meanwhile, the non-systematic variation near the leading-edge is the most sensitive, and it contributes to most of the performance disperse but only accounts for a geometric variation of about 0.45%.

Keywords: manufacture variations; uncertainty quantification; robust design; sensitive analysis; axial compressor

Citation: Liu, B.; Liu, J.; Yu, X.; An, G. A Novel Decomposition Method for Manufacture Variations and the Sensitivity Analysis on Compressor Blades. *Aerospace* **2022**, *9*, 542. https://doi.org/10.3390/aerospace9100542

Academic Editor: Christian Breitsamter

Received: 3 August 2022
Accepted: 19 September 2022
Published: 23 September 2022

Publisher's Note: MDPI stays neutral with regard to jurisdictional claims in published maps and institutional affiliations.

1. Introduction

Geometric variations between the manufactured or in-service blades and the ideal designed blade are inevitable and have a significant effect on the aerodynamic performances of blade profiles or compressors or even other turbomachines. As summarized by Wong et al. [1], the manufacturing variations in a compressor of a jet engine could cause a 10% loss in blade incidence range, i.e., a significant degradation of compressor stall margin, and a 4% increase in loss, corresponding to 1~2% degradation of compressor efficiency. Hence, in recent years, the study of the influence of manufacture variations on aero-engine compressors has been widely concerned [2–5].

Generally, the manufacture variation related researches could be divided into two categories, i.e., geometric uncertainty quantification (UQ) analysis and robust design analysis [6]. The UQ analyses mainly concern the aerodynamic change with the variation

of blade geometric variations [7–11], however, the robust design studies focus on the blade design optimization to the goal of geometric variation insensitivity [12–16].

For both the UQ analysis and robust design study, blades with geometric variations should be generated at first, hence the accurate modeling of geometric variations shall always be a key process to guarantee the reliability of the research. There are four representative methods to modeling the geometric variations: (1) a supposed geometric tolerance method, such as the Hicks–Henne bump method [13,17], in which manufacture variations are modeled as superposing a Hicks–Henne like smooth perturbation along the blade surface; (2) blade surface point driving method [1,12], in which representative blade surface points are moved to model the small geometry variations; (3) blade geometric design parameter variation method [10,11,18,19], in which blade design parameters, such as the blade chord length, the maximum thickness, the thickness of blade leading-edge, and even the blade metal angles are changes in a range according to the real measured blades; and (4) orthogonal decomposition method based eigenmode extraction methods, such as Principal Component Analysis (PCA) method [8,20–22], in which the complicated real measured blade geometry variations are reduced into some typical variation modes. For the above-mentioned geometric modeling methods, features of geometric variations should always be determined based on real manufacture variations, such as the magnitude of the profile tolerance and the statistical distribution characteristics of the manufacture variations. For real geometry variations, the normal distribution could be a reasonable approximation; however, the variation distribution along the blade surface is very complicated and may have no regular pattern [23]. Hence, these four types of modeling methods should be carefully validated at first. Moreover, because of significant nonlinear effects for the geometric variations on the blade aerodynamic performance [24,25], the accuracy of the geometric modeling shall be evaluated based on blade performance uncertainty features. Hence, some performance based geometry modeling methods were proposed recently, such as the active subspace method [1,26], in which the main variation modes, as extracted based on PCA or Karhunen–Loeve (K-L) expansion [27] methods, are validated further by the impact of performance gradient.

The accurate modeling of the manufactured geometric variations is very important for both UQ analyses and robust design studies. If the manufacture variations are modeled not accurately enough, the UQ analysis and the robust design results may not be credible enough to reflect the effects of real geometry variation. For example, the published studies on geometric sensitivity analyses are usually implemented based on deterministic local blade geometry variations; however, the real geometry variations could occur on the whole of the blade surface with some random features, leading to the very complicated correlation effect for geometry variations at different locations [28], which is rarely considered by traditional manufacture variation modeling methods. Unfortunately, few studies are concerned with this problem. Generally speaking, there are two limitations for accurate modeling of the manufacture variations: (1) the lack of real measured data with sufficient samples to statistical the manufacture variations at different blade locations and their correlations and (2) the lack of an appropriate variation decomposition method to decompose the manufacture variations into variations which could be modeled by reduced order methods or not.

In the present work, real manufacture variations obtained from 100 measured blades for an outer stage of a high-pressure compressor are analyzed in detail. A novel variation decomposition method is developed to decompose the variations into systematic variation and non-systematic variation parts. The systematic variation could be considered as the manufacture uncertainty of the blade geometry design parameters, while the non-systematic part could deal with some tiny variations which could barely be modeled based on traditional methods. In order to provide some guidance for the modeling of manufacture variations, the statistical characteristics of different types of variations are analyzed.

Then, to clarify whether the small-scale non-systematic part could be omitted or not during the variation modeling, blade performance statistical analysis and sensitivity analysis are also conducted for different types of variations.

2. Decomposition Method for Manufacture Variations

The nominal blade used in the present work is a mid-section of a rotor blade in an outer stage of a high-pressure compressor (inlet Mach number Ma_{in} = 0.5, Reynolds number Re = 1.0 × 10^6, inlet turbulence Tu = 4%, AVDR = 1.0, solidity = 1.12), which has been manufactured by a numerical control machining process and finished using vibratory polishing to improve the surface roughness. A set of 100 newly manufactured blades was measured, and all the measured blade data are shown in Figure 1. It should be noted that, as shown in Figure 1, the mean blade (blue line) does not coincide with the nominal blade. This indicates that the mean value of manufacture variations in this study is not zero.

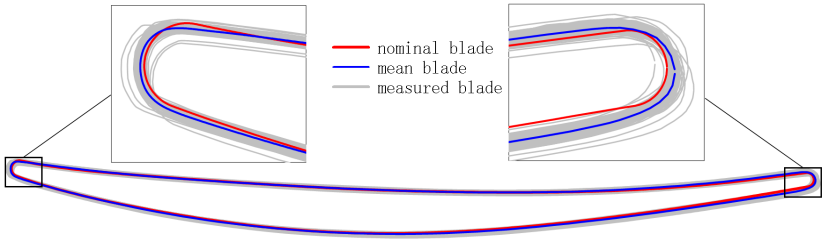

Figure 1. Nominal blade (red), measured blades (grey), and mean blade (blue) of the mid-height section from a high-pressure compressor rotor outlet stage.

2.1. Definition of Manufacture Variations

As shown in Figure 2a, the manufacture variation ε is defined as the distance from the nominal blade (red) to the measured blade (black) in the normal direction **n** at the arc-length s on the nominal blade profile. When the profile of the measured blade locates outside the nominal blade, the manufacture variation is positive (red shades). The negative deviation is depicted with blue shades, which can also be seen in Figure 2b. Thus, the measured blade profile $\mathbf{x}_{mea}$ is constructed from the nominal blade and the manufacture variation ε as

$$\mathbf{x}_{mea}(s) = \mathbf{x}_{nom}(s) + \mathbf{n}(s)\varepsilon_{mea}(s) \quad (1)$$

where $\mathbf{x}_{nom}$ is the profile coordinate vector of the nominal blade at the arc-length s, **n** is the corresponding normal vector, and $\mathbf{x}_{mea}$ is the profile coordinate vector of the measured blade.

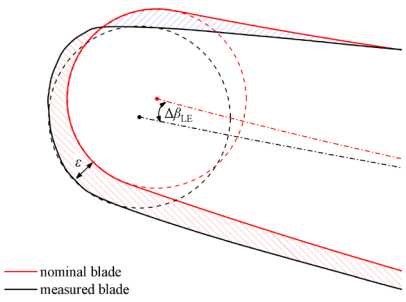

(**a**) Measured and nominal blade profile near LE

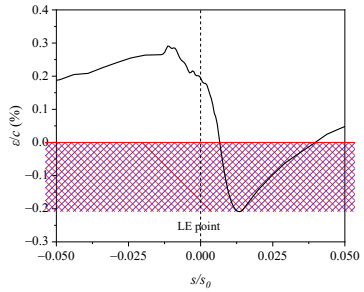

(**b**) Manufacture variation near LE

Figure 2. Representative manufacture variation between the measured and nominal blades.

Figure 2b shows the manufacture variation of a certain measured blade near the leading-edge (LE), in which the abscissa s/s_0 represents the normalized arc-length and the ordinate represents the manufacture variation ε nondimensionalized by blade chord length c. The corresponding blade profile is shown in Figure 2a. It can be seen from the figure that the centerline of the measured blade is changed relative to the nominal blade due to the manufacture variation, which means the inlet metal angle (β_{LE}) of this measured blade is different from the nominal blade. Meanwhile, the LE shape of the measured blade deviates from the circle by comparing the profile line (black solid line) with the fitting circular line (black dotted line). This indicates that the manufacture variation has two effects on the blade profile:

1. Systematically changed the profile parameters of the blade, such as the inlet metal angle and the chord length;
2. Deformed the local geometric profile of the blade.

On this basis, the manufacture variation could be decomposed into **systematic variation** and **non-systematic variation**.

2.2. Systematic Manufacture Variation

In order to evaluate the systematic variation of the blade, this study parameterizes the blade profile as profile parameter vector **p** (Equation (2)). The profile parameters used in this paper are shown in the Table 1.

Table 1. Profile parameters for the systematic variation.

Symbol	Profile Parameters
λ	Stagger angle
c	Chord length
r_{LE}, r_{TE}	Radius of LE and trailing-edge (TE)
t_{max}	Maximum thickness
β_{LE}, β_{TE}	Inlet and outlet metal angle

$$\mathbf{p} = [\lambda, c, \beta_{LE}, \beta_{TE}, r_{LE}, r_{TE}, t_{max}] \quad (2)$$

The systematic variation is defined as the difference of the above parameters between the measured and the nominal blades:

$$\Delta\mathbf{p} = \mathbf{p}_{mea} - \mathbf{p}_{nom} = [\Delta\lambda, \Delta c, \Delta\beta_{LE}, \Delta\beta_{TE}, \Delta r_{LE}, \Delta r_{TE}, \Delta t_{max}] \quad (3)$$

The above profile parameters were obtained by reverse fitting extraction from the nominal and measured blades. The parameter definitions are shown in Figure 3. The parameter extraction method references Lang's work [18]. The centerline was obtained by solving the tangent circle of the blade profile, and the blade thickness was determined by the radius of the tangent circle. The camber angle of the centerline is defined as the angle between the tangent line of the centerline and the abscissa, and it is normalized by the inlet and outlet metal angle. Therefore, the centerline can be determined by the inlet and outlet metal angle and the normalized camber angle distribution. Similarly, the thickness distribution was piecewise normalized by the maximum thickness and the radius of LE and TE. The blade thickness can be also determined by the above parameters and the normalized thickness distribution. Therefore, the profile of the nominal blade could be determined by the profile parameter vector **p** without changing the normalized camber angle distribution of the centerline and the normalized thickness distribution in the design system, as shown in Equation (4).

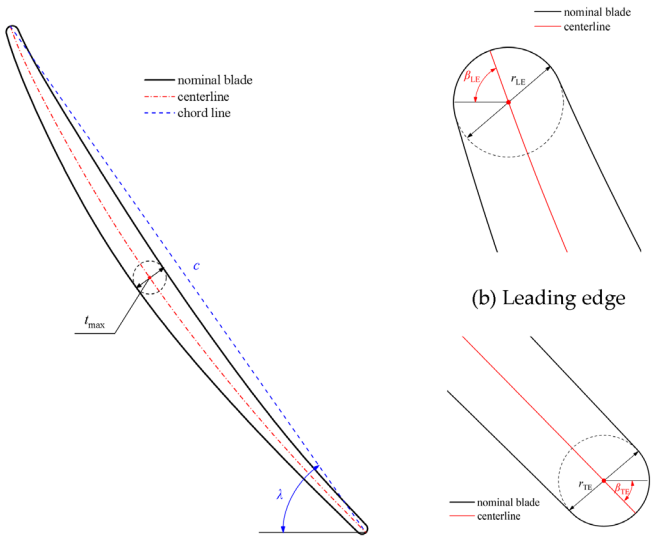

(a) Blade profile (b) Leading edge (c) Leading edge

Figure 3. Profile parameters definition.

$$\mathbf{x}_{nom} = f(\mathbf{p}_{nom}) = f([\lambda, c, \beta_{LE}, \beta_{TE}, r_{LE}, r_{TE}, t_{max}]_{nom}) \quad (4)$$

Due to the small magnitude of the manufacture variation, high accuracy of blade profile parameter extraction is required. Meanwhile, the measured blade profile has some disadvantages, such as the discontinuity of the curve, as shown in Figure 2, which makes it difficult to improve the extraction accuracy. Therefore, the accuracy of the parameter extraction method adopted in this paper has been verified.

More than 100 sets of the blade with known parameters were selected to verify the extraction method. The accuracy verification results are shown in Table 2, where std means standard deviation. The parameters related to geometric dimensions, such as the chord length and the radii of the LE and the TE, are percentages relative to themselves.

Table 2. The profile parameters extraction error.

Profile Parameters	Extraction Error (Mean ± 2std)
Stagger angle (°)	0.005 ± 0.008
Chord length (%)	0.002 ± 0.002
Inlet metal angle (°)	−0.005 ± 0.006
Outlet metal angle (°)	−0.002 ± 0.011
Radius of LE (%)	0.001 ± 0.001
Radius of TE (%)	0.001 ± 0.001
Maximum thickness (%)	0.012 ± 0.063

It can be seen that the extraction errors of all parameters are very small. Taking the stagger angle λ as an example, the extraction error is centered on the mean value of 0.005°, and the dispersion (with double standard deviation as the evaluation criterion) is ±0.008°. Similar to the stagger angle, the mean value and the standard deviation of other parameters are close to zero. Even for the maximum thickness with the largest error, the mean extraction error is only 0.012% and the dispersion is only 0.063%. Therefore, the extraction method in this paper meets the research needs of the systematic variation.

2.3. Non-Systematic Manufacture Variation

The extraction of non-systematic variation is based on the systematically reconstructed blade. The non-systematic variation ε_{non} is defined as the distance between the systematically reconstructed blade and the corresponding measured blade, which can be expressed as

$$\mathbf{x}_{mea}(s) = \mathbf{x}_{sys}(s) + \mathbf{n}(s)\varepsilon_{non}(s) \quad (5)$$

According to Equation (4), the nominal blade profile can be determined by the profile parameter vector $\mathbf{p}_{nom}$. Similarly, the blade profile with systematic variation, i.e., systematically reconstructed blade, can also be reconstructed by $\mathbf{p}_{nom}$ and $\Delta\mathbf{p}$:

$$\mathbf{x}_{sys} = f(\mathbf{p}_{nom} + \Delta\mathbf{p}) \quad (6)$$

Figure 4 shows an example of the above approach. In this figure, the blue line is the systematically reconstructed blade, which is reconstructed from the systematic variation extracted from the corresponding measured blade (black line). As can be seen in Figure 4, the systematically reconstructed blade has a different β_{LE} and r_{TE} relative to the nominal blade. It also has non-systematic variations (red and blue shades) relative to the corresponding measured blade.

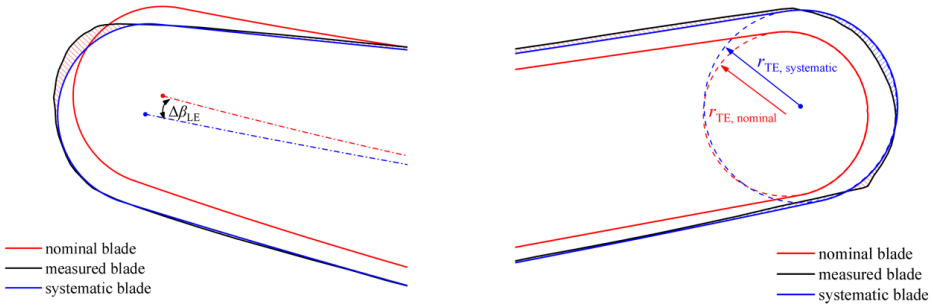

(**a**) LE (**b**) TE

Figure 4. Example of the systematic blade and non-systematic variation on the blade profile.

In summary, the calculation process of non-systematic variation is shown in Figure 5, which is briefly described below:

- Step 1: Extract systematic variations $\Delta\mathbf{p}$;
- Step 2: Use parametric modeling to reconstruct the systematic blade profile $\mathbf{x}_{sys}$;
- Step 3: Calculate the variation ε_{non} between the systematic blade and the corresponding measured blade.

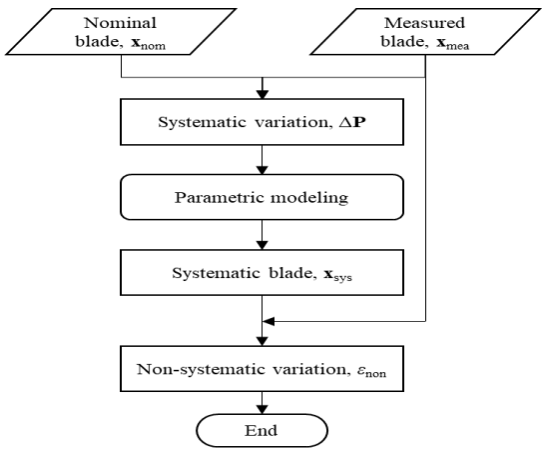

Figure 5. Flowchart for calculating the non-systematic variation.

Figure 6 presents a comparative example of the manufacture variation ε_{mea} and the non-systematic variation ε_{non} obtained by the above method for a certain measured blade. The abscissa s/s_0 represents the normalized arc-length, $s/s_0 < 0$ means the suction surface and, otherwise, the pressure surface. It can be seen that the non-systematic variation is closer to zero than the manufacture variation. The maximum values of both are located near LE, while the non-systematic variation is about 40% of the manufacture variation. The corresponding deformation of the LE geometry caused by the non-systematic variation is shown in Figure 4a, i.e., the discrepancy between the measured blade and the systematic blade. Since the systematic blade is reconstructed by using high-precision systematic variation, which is very close to the measured blade, the non-systematic variation can indicate the local geometric variation of the measured blade profile (especially the asymmetry of shapes of the LE and the TE).

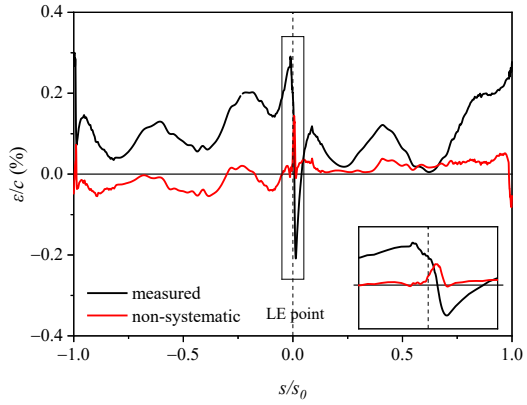

Figure 6. Comparison of the measured and non-systematic variations.

3. Statistic Characteristics for Different Type of Manufacture Variation

By decomposing the manufacture variations into systematic and non-systematic variations, the effect of manufacture variations on blade profile can be demonstrated from two different aspects. The statistical characteristics of systematic and non-systematic variations are shown below.

3.1. Systematic Maufacture Variation

As mentioned above, at least 100 sets of newly manufactured blades were measured in this study, and the manufacture variations of all blades were decomposed using the above method. The systematic variation matrix $\Delta\mathbf{P}$ of measured blades has been obtained as

$$\Delta\mathbf{P} = \begin{bmatrix} \Delta\lambda_1 & \Delta c_1 & \cdots & \Delta t_{\max,1} \\ \Delta\lambda_2 & \Delta c_2 & \cdots & \Delta t_{\max,2} \\ \vdots & \vdots & & \vdots \\ \Delta\lambda_n & \Delta c_n & \cdots & \Delta t_{\max,n} \end{bmatrix} \tag{7}$$

where n is the total number of the measured blades.

Table 3 shows the statistical results of the systematic variation matrix $\Delta\mathbf{P}$. As shown in Table 3, the mean $\Delta\lambda$ is close to zero, and the dispersion (2std) is far less than $\Delta\beta_{LE}$ and $\Delta\beta_{TE}$. The mean value and dispersion of $\Delta\beta_{LE}$ and $\Delta\beta_{TE}$ are obviously larger. The dispersion of the $\Delta\beta_{TE}$ is greater than $\Delta\beta_{LE}$, and the mean value of the $\Delta\beta_{LE}$ is greater than $\Delta\beta_{TE}$. It is worth noting that the |mean/2std| of the $\Delta\beta_{LE}$ is equal to 1.67, which indicates that β_{LE} of all the measured blades is significantly large. The mean value and dispersion of Δc and Δt_{max} are small. Δr_{LE} has a large dispersion. The mean value of Δr_{TE} makes the trailing-edge obviously thicker, while the dispersion of Δr_{TE} is significantly large. In summary, on

average, systematic variations mainly lead to larger inlet and outlet metal angle of measured blades, a thinner leading-edge, and a thicker trailing-edge.

Table 3. Systematic variations of measured blades.

Delta Profile Parameters	Mean ± 2std	|Mean/2std|	*p*-Value *
$\Delta\lambda$ (°)	−0.01 ± 0.45	0.02	0.91
Δc (%)	0.29 ± 0.30	0.96	0.76
$\Delta\beta_{LE}$ (°)	3.31 ± 1.98	1.67	0.77
$\Delta\beta_{TE}$ (°)	2.10 ± 3.35	0.63	0.27
Δr_{LE} (%)	−2.00 ± 11.40	0.18	1.00
Δr_{TE} (%)	11.90 ± 16.54	0.72	1.00
Δt_{max} (%)	0.34 ± 2.50	0.13	0.75

* Kolmogorov–Smirnov test [29].

In addition to the mean value and standard deviation, the distribution form of variations is also important, therefore the Kolmogorov–Smirnov test for systematic variations is carried out. As shown in Table 3, the *p*-values of all systematic variations are significantly greater than 0.05, which means they all belong to normal distribution at a confidence level of 95% [29].

To further illustrate the distribution characteristics of systematic variations, a quantile–quantile (Q-Q) plot is drawn in Figure 7 [30]. Figure 7a shows the Q-Q plot of $\Delta\beta_{LE}$, the abscissa is the actual measured value of $\Delta\beta_{LE}$, and the ordinate is the fitting value of the normal distribution. The closer the points in the figure are to the reference line y = x (red line), the closer the distribution is to the normal distribution. In Table 3, the *p*-value of $\Delta\beta_{LE}$ is 0.77, and the points in Figure 7a are all near the reference line, indicating that the distribution of $\Delta\beta_{LE}$ is indeed close to the normal distribution. Meanwhile, although the p-value of $\Delta\beta_{TE}$ is only 0.27, most points in Figure 7b are also near the reference line, which proves that $\Delta\beta_{TE}$ also roughly meets the normal distribution.

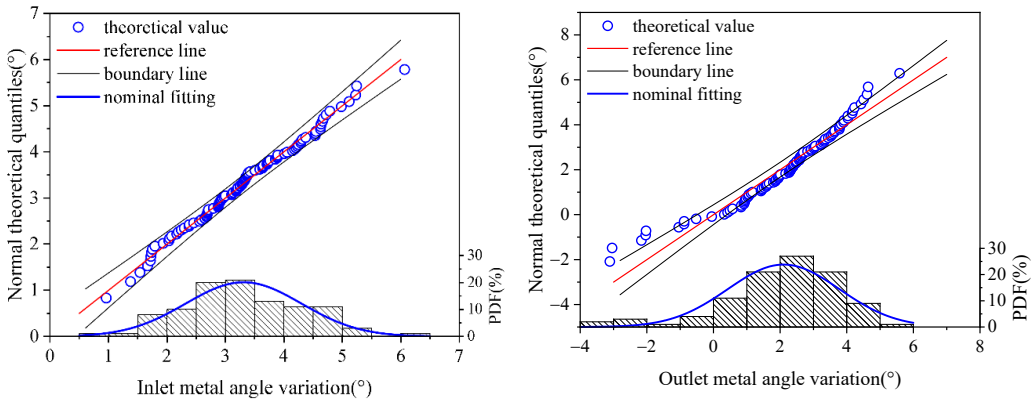

(**a**) $\Delta\beta_{LE}$ (**b**) $\Delta\beta_{TE}$

Figure 7. Quantile–quantile plot for systematic variations.

3.2. Non-Ystematic Maufacture Variation

By using the method suggested in Section 2, the non-systematic variation with the systematic variation excluded can be obtained for any measured blade. This section aims to present the statistical characteristics of the non-systematic variations.

Figure 8a shows the comparison between the manufacture variation and the non-systematic variation in normalized arc-length coordinates, where the red shades represent the double std of the non-systematic variations and the black shades represent that of the

manufacture variations. As shown in Figure 8a, the mean value of non-systematic variations is closer to zero and less dispersed than manufacture variations. On average, the std of non-systematic variations is about 40% of the manufacture variations. Figure 8b shows the comparison with the mean variation superposed on the nominal blade profile. It can be seen that the mean manufactured blade still increases the inlet metal angle at the LE, while the mean value of the non-systematic variation is close to zero, and only changes the shape of the LE of the blade profile locally.

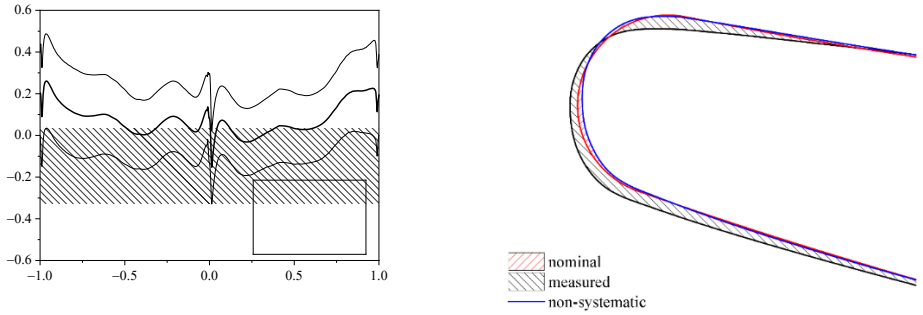

(**a**) Mean value and double std of variations (**b**) Mean variations on blade profile near LE

Figure 8. Comparison of the statistical characteristics between the manufacture and non-systematic variations.

4. Effect of Manufacture Variations on Blade Aerodynamic Performances

This section aims to obtain the statistical characteristics for the influence of manufacture variations on blade aerodynamic performance, and further to obtain that of the systematic and non-systematic variations on blade performance after the variation decomposition and, on this basis, to determine the difference and connection between them.

4.1. Computational Method

Numerical simulation was used to determine the influence of manufacture variations on blade aerodynamic performances. The flow solutions were calculated using the Multiple Blade Interacting Stream-tube Euler Solver (MISES) code, which was developed by Mark Drela in MIT [31,32]. In MISES, the inviscid, steady Euler equations on a two-dimensional H-grid with a coupled integral compressible boundary layer were calculated. The grid dynamically adapts to the solution ensuring that side edges of any element are on streamlines. In addition, the first grid point adjacent to the surface is located at the displacement thickness of the boundary layer away from the wall. MISES is very easy to use, has been extensively calibrated in subsonic and transonic flows [24,33], and it possesses the characteristics of fast calculation speed and high accuracy. Therefore, MISES has been widely used in the study of the blade geometric variations [17,27].

The computational grid settings are shown in Table 4, and the transition model in this paper was the modified Abu-Ghannam–Shaw bypass transition model. Figure 9 shows the comparison of MISES computational results and experimental results for different LE geometries [34]. The static pressure rise coefficient Cp is defined as

$$Cp = \frac{p - p_{\text{in}}}{p_{0,\text{in}} - p_{\text{in}}} \tag{8}$$

where $p_{0,\text{in}}$ represents the total pressure evaluated at blade row inlet, p_{in} represents the static pressure evaluated at blade row inlet, and p represents the local static pressure. It can be seen that MISES can well simulate the effect of small geometric variations on the flow details of blade surface.

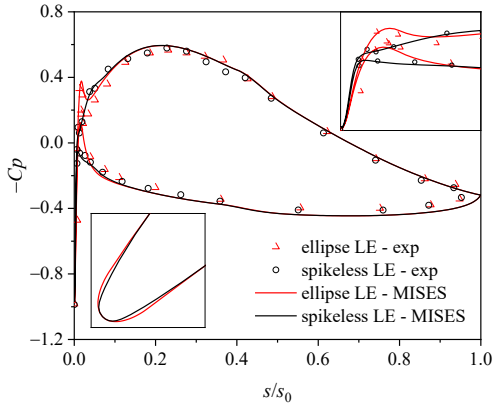

Figure 9. Comparison of blade surface pressure coefficient distribution on blade surface and near leading-edge region.

Table 4. MISES grid parameters.

Grid Parameters	Settings
Local/average spacing ratios at LE, TE	0.1, 0.9
Type of grid topology at inlet and outlet grid	Both the periodic H-type grid
Number of inlet points	50
Number of outlet points	30
Number of streamlines	20

4.2. Statistic Characteristics of the Influence of Manufacture Variations

Figure 10a presents the profile loss characteristics of the nominal blade and all the measured blades, as well as the mean value and std for the profile losses of the measured blades at each inlet flow angle. The profile loss coefficient was defined as

$$\omega = \frac{p_{0,in} - p_{0,out}}{p_{0,in} - p_{in}} \quad (9)$$

where $p_{0,\mathrm{in}}$ represents the total pressure evaluated at blade row inlet, $p_{0,\mathrm{out}}$ represents the total pressure evaluated at blade row outlet, and p_{in} represents the static pressure evaluated at blade row inlet. It can be seen from Figure 10a that the dispersion (2std) of the profile loss is the minimum at the inlet flow angle with the minimum profile loss. The inlet flow angle with the minimum loss of the nominal blade is defined as the reference inlet flow angle α_{ref}, the corresponding loss as the reference loss $\omega_{\mathrm{reference}}$, and

$$\omega_{\mathrm{rel}} = \omega/\omega_{\mathrm{reference}} \quad (10)$$

What is more noteworthy in Figure 10a is that, under the condition of positive inlet flow angle, not only is the mean loss of the measured blade greater than that of the nominal blade, but almost all the measured blades have greater losses. Similarly, under the condition of negative inlet flow angle, the mean loss and almost all the measured blade profile losses are smaller than the nominal blade. This indicates that the losses of the measured blades are systematically deviated from the nominal blade due to manufacture variations.

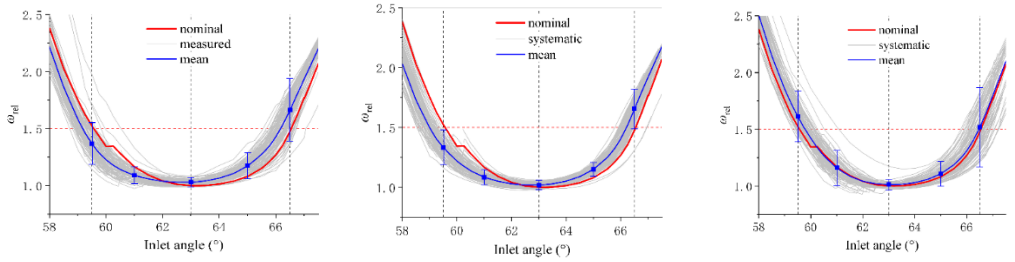

(**a**) Measured blades (**b**) Systematic blades (**c**) Non-systematic blades

Figure 10. Effect of the variations on the blade profile loss.

Figure 10b presents the loss characteristics of systematic blades, which were decomposed and reconstructed by the corresponding manufacture variations. It presents the influence of systematic variations on the blade profile loss. It can be seen from the figure that the influence of systematic variation is similar to that of the whole manufacture variation, that is, the blade profile loss is systematically increased under the condition of positive inlet flow angle, while it is opposite under the negative inlet flow angle. Associating with the characteristics of the systematic variation in Table 3, this is possibly because the mean value of systematic variation also deviates significantly from the nominal blade (especially the inlet metal angle). This correlation will be discussed in a later section.

Figure 10c shows the loss characteristics of non-systematic blades, which were obtained by superimposed the corresponding non-systematic variations on the nominal blade profile. It can be seen from the figure that the mean loss of non-systematic blades almost coincides with the nominal blade, but the dispersions (2std) of the positive and negative inlet flow angle are much higher than that of systematic blades.

In order to further illustrate the above characteristics, the loss statistical characteristics of variation blades are exhibited in Figure 11. The negative/positive range is defined as the condition in which the loss is 1.5 times the reference loss [17].

Figure 11 illustrates the mean and std of the difference between variation blades and the nominal blade. The $\Delta\omega_{rel}$ is defined as:

$$\Delta\omega_{rel} = \omega_{rel,\ variation} - \omega_{rel,\ nominal} \quad (11)$$

where $\omega_{rel,\ variation}$ can be the relative loss of measured, systematic, and non-systematic blades. When $\Delta\omega_{rel}$ equals zero, it means that the loss of the variation blade is equal to the nominal blade.

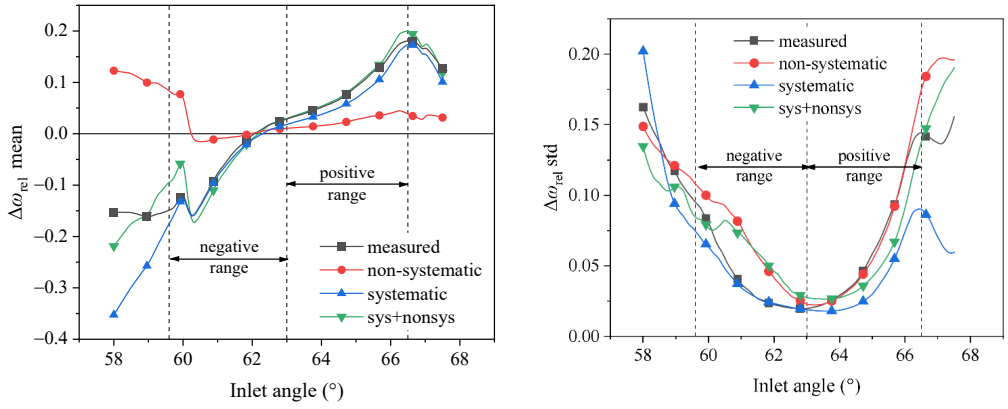

(**a**) Mean value of $\Delta\omega_{rel}$ (**b**) Std of $\Delta\omega_{rel}$

Figure 11. Statistical characteristics for the effect of the variations on the blade profile loss.

Figure 11a presents the mean $\Delta\omega_{rel}$ of variation blades. The following characteristics can be seen from the figure:

1. When the inlet flow angle $\alpha_{in} > 60°$, the mean $\Delta\omega_{rel}$ of systematic blades is basically consistent with that of measured blades;
2. When the inlet flow angle $\alpha_{in} < 60°$, the mean $\Delta\omega_{rel}$ of systematic blades deviates from that of measured blades.
3. When the inlet flow angle $\alpha_{in} > 60°$, the mean loss of non-systematic blades approximates to that of the nominal blade. When $\alpha_{in} < 60°$, it deviates from that of the nominal blade.

In summary, it can be considered that the systematic ω_{rel} deviation of measured blades described above is caused by systematic variations in most inlet flow angle conditions.

Figure 11b presents $\Delta\omega_{rel}$ std of variation blades. The following characteristics can be seen from the figure:

4. $\Delta\omega_{rel}$ std of measured blades in the positive range is approximately coincident with that of non-systematic blades, and is about twice the std of systematic blades.
5. $\Delta\omega_{rel}$ std of measured blades in the negative range is closer to that of systematic blades, while the std of non-systematic blades is obviously larger.

To sum up, in the positive range, the non-systematic variation determines the loss dispersion of the variation blades, while in the negative range, the loss dispersion is closer to that caused by systematic variations.

On this basis, in order to verify whether the effects of systematic and non-systematic variations on losses can be linearly superimposed, the loss deviations of each systematic and non-systematic blade were processed as:

$$\Delta\omega_{rel,\,(systematic\,+\,non\text{-}systematic),\,i} = \Delta\omega_{rel,\,systematic,\,i} + \Delta\omega_{rel,\,non\text{-}systematic,\,i} \quad (12)$$

where $\Delta\omega_{rel,\,sys,\,i}$ represents the loss deviation of the systematic blade No. i, and $\Delta\omega_{rel,\,non,\,i}$ represents the loss deviation of the corresponding non-systematic blade. Therefore, $\Delta\omega_{rel,\,(sys\,+\,non),\,i}$ represents the linear superposition of the loss deviation between the systematic blade and the corresponding non-systematic blade. The mean value and the std of $\Delta\omega_{rel,\,(sys\,+\,non)}$ have been illustrated in Figure 11 (green line).

It can be seen from Figure 11 that the mean loss deviation of the linear superposition is consistent with that of the measured blade when the inlet flow angle is greater than 60°. However, the std obtained by the linear superposition is different from that of the measured blade. Therefore, the effects of systematic and non-systematic variations on blade losses have a weak linear additivity, which requires further modification and research.

In conclusion, systematic variations mainly determine the mean loss deviation of blades, while non-systematic variations have a large impact on the loss dispersion. Therefore, the influences of these two decomposition variations will be respectively described below.

4.3. Blade Design Parameter Based Sensitivity Analysis for Systematic Variations

As shown in Table 3, seven parameters were parameterized for the blade profile when extracting systematic variation. Therefore, systematic variation is further decomposed into variations of these seven independent parameters in this section.

Table 5 shows the range selected when each systematic variation parameter is changed independently. Based on this, the loss of a series of variation blade is calculated. Similar to other researchers' studies, the effect of these parameters on profile loss has strong linear characteristics [10,11,18,19]. Therefore, in order to avoid redundancy, only the most remarkable influence parameter of inlet metal angle variation is presented in Figure 12.

Table 5. Selected range for the independent parameters of the systematic variation.

Delta Profile Parameters	Top and Bottom Limitation
$\Delta\lambda$ (°)	−0.5~+0.5
Δc (%)	−0.63~+0.6
$\Delta\beta_{LE}$ (°)	−5.0~+5.0
$\Delta\beta_{TE}$ (°)	−5.5~+5.5
Δr_{LE} (%)	−13.8~+13.8
Δr_{TE} (%)	−31.1~+31.1
Δt_{max} (%)	−2.9~2.9

Figure 12a is the schematic diagram of the blade profile with the changing of the inlet metal angle, where +5° represents that the blade profile is bent 5° to the suction surface. Figure 12b shows the variation rule of $\Delta\omega_{rel}$ with $\Delta\beta_{LE}$ at the selected three inlet flow angles, which α_{in} = 59.6° means that the inlet flow angle is at the negative incidence limit, and α_{in} = 63.0° means the minimum loss condition, and α_{in} = 66.5°, positive incidence limit. It can be seen from Figure 12b that, as mentioned above, $\Delta\omega_{rel}$ has a strong linear effect with the change of $\Delta\beta_{LE}$.

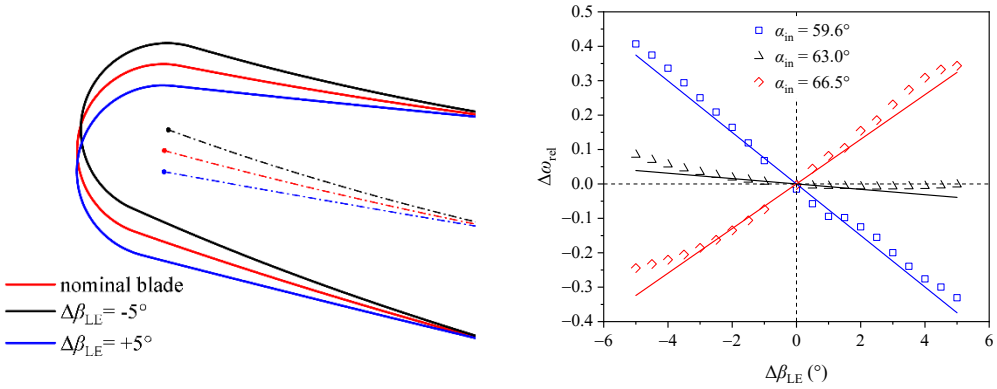

(**a**) Blade profile near LE (**b**) $\Delta\omega_{rel}$ in different α_{in} conditions

Figure 12. Effect of inlet metal angle variations on blade profile and profile losses.

On this basis, the sensitivity analysis is conducted on the profile loss to each systematic variation at several inlet flow angles, and the results are shown in Table 6. The "before regression" line indicates the sensitivity obtained by independently changing the systematic variation parameters. The "post regression" line indicates the sensitivity of correction using linear regression, i.e., by using least square fitting for all the sensitivity coefficients.

Table 6. Sensitivity of the profile loss to the systematic variations (before or after regression).

Inlet Flow Angle Condition	Regression or Not	$\Delta\beta_{LE}$	$\Delta\beta_{TE}$	$\Delta\lambda$	Δc	Δr_{LE}	Δr_{TE}	Δt_{max}
α_{in} = 63.0° sensitivity	before regression	−0.009	0.000	0.036	0.018	0.427	0.871	0.043
	post regression	0.000	0.001	−0.009	−0.046	0.574	0.852	0.051
α_{in} = 59.6° sensitivity	before regression	−0.074	0.005	0.394	0.050	2.191	1.387	0.006
	post regression	−0.048	0.003	−0.105	−0.215	5.543	0.621	−1.139
α_{in} = 66.5° sensitivity	before regression	0.059	0.000	−0.351	−0.026	−1.075	−0.410	−0.268
	post regression	0.065	0.007	0.038	−0.381	2.093	−0.352	−1.346

After obtaining the sensitivity of the profile loss to each systematic variation parameter, the sensitivity can be used to estimate the profile loss:

$$\Delta\omega_{\mathrm{rel,estimate}} = k_1\Delta\lambda + k_2\Delta c + k_3\Delta\beta_{\mathrm{LE}} + k_4\Delta\beta_{\mathrm{TE}} + k_5\Delta r_{\mathrm{LE}} + k_6\Delta r_{\mathrm{TE}} + k_7\Delta t_{\max} \quad (13)$$

where the k_i represents the sensitivity in Table 6.

Through Equation (13) and the extracted value of the systematic variations, the profile loss of each systematic blade can be estimated, thus obtaining Figure 13. The abscissa is the calculated value of the loss deviation for each systematic blade, and the ordinate is the estimated value using Equation (13). The red line is the result of the linear fitting, and R^2 is the coefficient of determination. As can be seen from the fitting results in Figure 13, there is a certain linear relationship between the loss deviation estimated by the sensitivity and that of systematic blades.

For instance, the coefficient $R^2 = 0.55$ when $\alpha_{\mathrm{in}} = 59.6°$, which means that at least 55% of the systematic loss deviation is determined by the linear superposition of parameter sensitivities. However, at the same time, it is worth noting that no matter the inlet flow angle state, the intercept of the fitting line is not zero, nor is the slope one. This indicates that although independent parameter sensitivities can indicate the trend of the systematic loss deviation, there are still some problems in quantitatively estimating the systematic loss deviation according to independent parameter sensitivities. There is a coupling relationship between each systematic variation parameters and therefore the sensitivity needs to be modified.

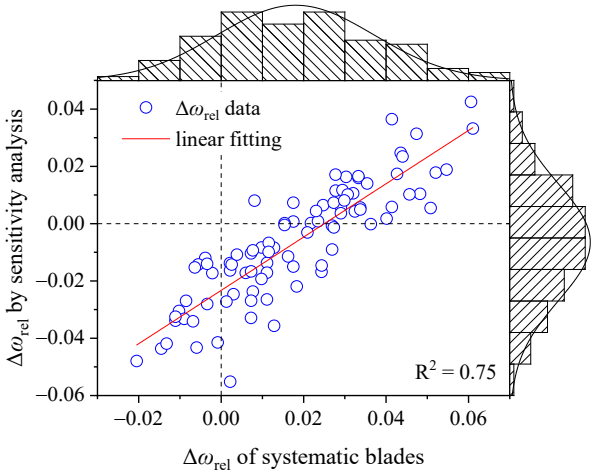

(**a**) $\alpha_{\mathrm{in}} = 63.0°$

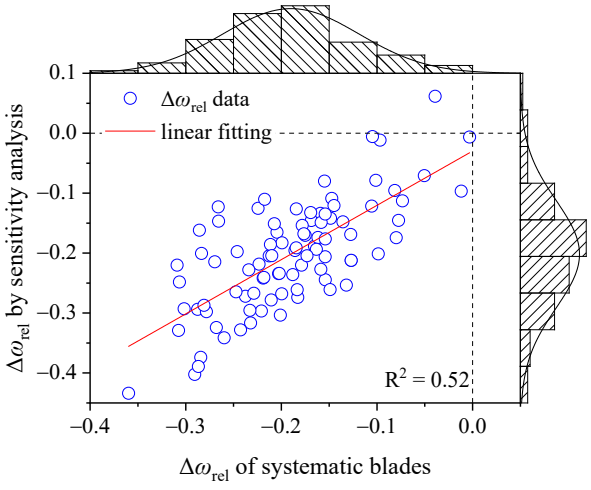

(**b**) $\alpha_{\mathrm{in}} = 59.6°$

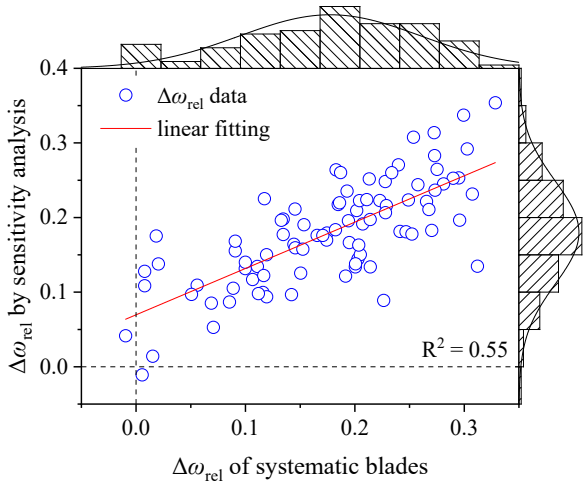

(**c**) α_{in} = 66.5°

Figure 13. The relationship between $\Delta\omega_{rel}$ obtained by the sensitivity analysis and $\Delta\omega_{rel}$ of systematic blades.

Because of a partial linear relationship between $\Delta\omega_{rel}$ of systematic blades and systematic variation parameters, which has been presented in Figure 13, based on Formula 12, a linear regression between $\Delta\omega_{rel}$ of systematic blades and systematic variation parameters based on Equation (13) is conducted, so as to modify the sensitivity of each parameter. The results of the linear regression are shown in Figure 14. The ordinate is $\Delta\omega_{rel}$ obtained by using linear regression relationship, and the red line is the y = x reference line. Meanwhile, sensitivities of systematic parameters obtained by linear regression are listed as "post regression" results in Table 6.

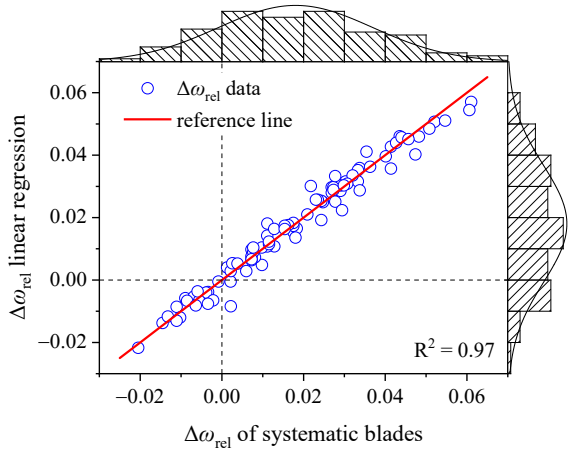

(**a**) α_{in} = 63.0°

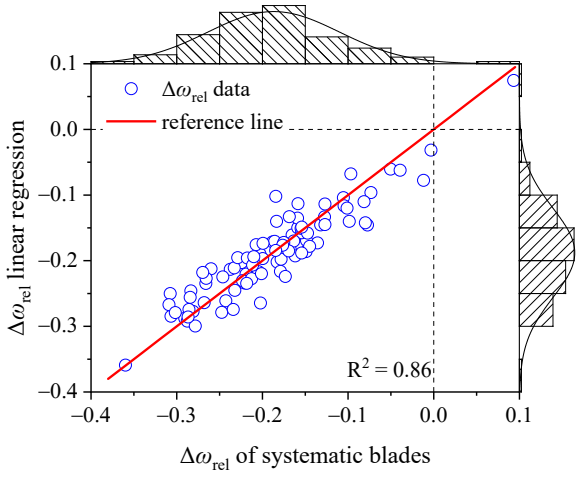

(**b**) α_{in} = 59.6°

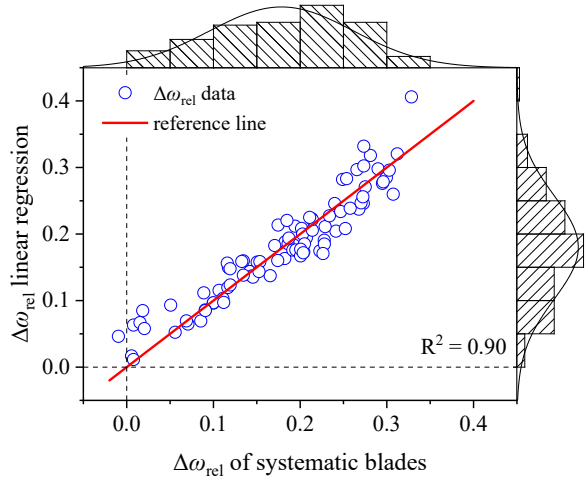

(**c**) α_{in} = 66.5°

Figure 14. Linear regression for $\Delta\omega_{rel}$ of systematic blades.

As shown in Figure 14, the estimation of $\Delta\omega_{rel}$ obtained by linear regression is not only close to y = x reference line, but also the correlation coefficient R^2 is greater than 0.85. Therefore, regression sensitivities of systematic variation parameters can be used to estimate the statistical characteristics of $\Delta\omega_{rel}$ of systematic blades [35].

The sensitivities of systematic variation parameters before and after regression are compared in Table 6. The sensitivity changes before and after regression represent the effect of the parameter coupling relationship. The remarkable characteristic of the coupling relationship is that the sensitivities of the inlet metal angle and the stagger angle are obviously reduced, and the sensitivities of the chord length, the radii of the LE and the TE, and the maximum thickness are improved.

Figure 15 presents the contribution of each systematic variation parameter to the mean value and std of $\Delta\omega_{rel}$ using the sensitivity obtained by linear regression. As can be seen from Figure 15a, the effect of the inlet metal angle on the mean $\Delta\omega_{rel}$ is much higher than that of other parameters. This is mainly because, as shown in Table 3, the mean variation of the inlet metal angle is very large, which can be seen from its |mean/2std| being much higher than other parameters.

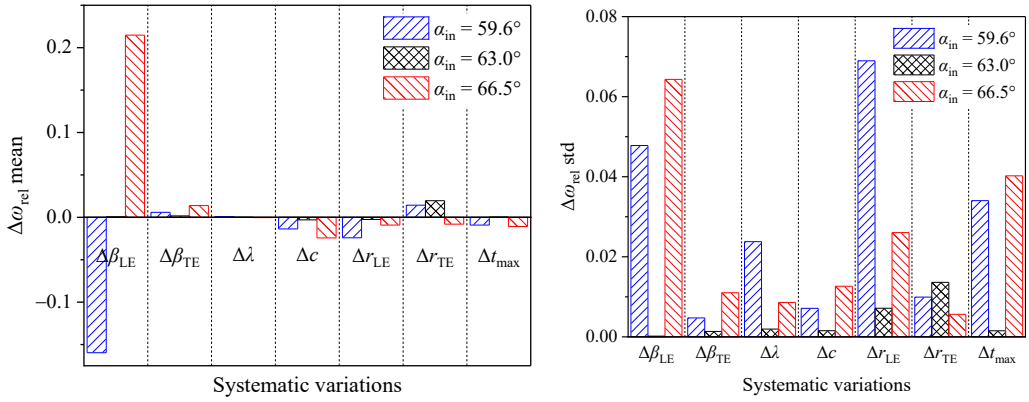

Figure 15. Effect of the $\Delta\omega_{rel}$ statistical characteristics to the systematic variations.

Meanwhile, it can be seen from Figure 15b that in the condition of α_{in} = 63.0°, the radius of the TE makes the largest contribution to $\Delta\omega_{rel}$ std. In other conditions, the contributions of the outlet metal angle, the chord length, and the radius of the TE to std are small, while the contributions of the inlet metal angle, the radius of the LE, and the maximum thickness are obviously larger than other parameters. It is also worth noting that when α_{in} = 59.6°, the contribution of the radius of the LE to std is even greater than that of the inlet metal angle.

Obviously, the contribution of systematic variations to the mean value and std of $\Delta\omega_{rel}$ is not only related to their sensitivities, but also directly related to their manufacture statistical characteristics. Thus, Figure 15 does not clearly indicate the comparison of the sensitivity between each of the systematic variation parameters.

At the same time, due to the different units of each systematic variation parameter, the sensitivity values in Table 6 have no comparative significance with each other. Therefore, in order to compare the sensitivity between each systematic variation parameter, the upper and lower limits that can be allowed in manufacture processing for each parameter are selected to evaluate the effect of each parameter on $\Delta\omega_{rel}$ std. Thus, Figure 16 is obtained.

Figure 16 shows that the radius of the TE is the most sensitive parameter when α_{in} = 63.0°. In other conditions, the inlet metal angle is the most sensitive parameter, especially in the condition of positive inlet angle of α_{in} = 66.5°. Its sensitivity is far greater than other parameters. Meanwhile, the sensitivities of the radius of the LE and the maximum thickness are obviously greater than other parameters. The sensitivity of the radius of the LE is relatively higher at α_{in} = 59.6°, i.e., at negative inlet flow angle condition.

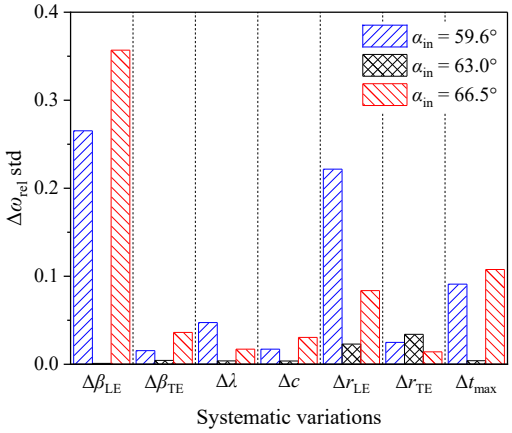

Figure 16. Sensitivity of $\Delta\omega_{rel}$ to systematic variations.

4.4. Region Decomposition Based Sensitivity Analysis for Non-Systematic Variations

Previous studies show that the manufacture variation of the LE has the most significant effect on the profile loss. In this section, the blade surface is further decomposed into different regions to reveal the effect of non-systematic variations on the profile loss at different locations. As shown in Figure 8a, the std of non-systematic variations has several "nodes" close to zero. Therefore, these "nodes" are used to divide the blade into eight regions as shown in Figure 17.

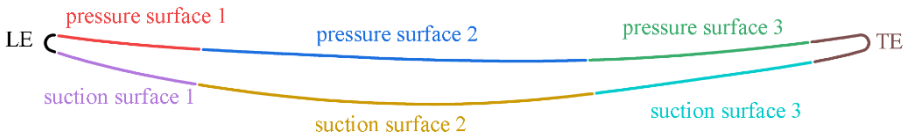

Figure 17. Schematic diagram of decomposing the blade profile.

The multipliers in Equation (14) were used to extract the non-systematic variations in different regions. The variations in each region were superimposed on the nominal blade profile, so as to obtain eight groups of variation blades. Each group of blades represents the non-systematic variations in its own region.

$$Multiper = \begin{cases} 1 & \text{inside the region} \\ 0 & \text{outside the region} \\ \text{smooth transition} & \text{region boundary} \end{cases} \quad (14)$$

Figure 18 shows the calculation results of the effect of non-systematic variations on the profile loss in different regions. And Figure 18a shows the effect of LE variations on the profile loss. It can be seen that, similar to the effect of the whole non-systematic variations, the mean loss caused by LE variations is approximately coincident with the loss of the nominal blade, and the std of the loss caused by the LE variation is large.

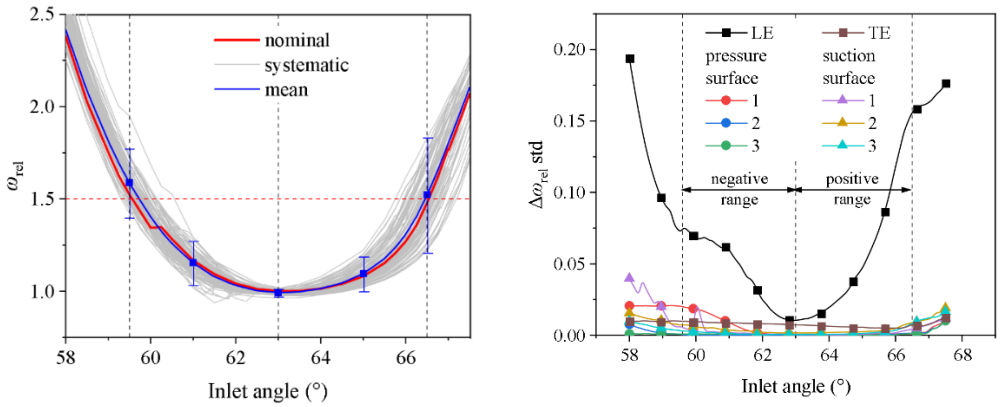

(**a**) Profile loss of blades with the LE variation (**b**) Std

Figure 18. Effect of non-systematic variations on the blade profile loss.

In addition to the LE region, the mean loss of non-systematic variations in other regions is also consistent with the loss of the nominal blade. $\Delta\omega_{rel}$ std due to non-systematic variations in each region is illustrated in Figure 18b. It can be seen that the std caused by LE variations is significantly greater than that of other regions. Thus, the profile loss is most sensitive to non-systematic variations in the LE region. It should be noted that, according to the std of non-systematic variations obtained in Figure 8a, the most sensitive LE region only accounts for a geometric variation of about 0.45%.

As shown in Figure 18b, $\Delta\omega_{rel}$ std generated by non-systematic variations in other regions is close to zero. On this basis, $\Delta\omega_{rel}$ std caused by non-systematic variations superimposed on the LE only and on the whole blade is compared in Figure 19. It can be seen that in the positive range, $\Delta\omega_{rel}$ std caused by the LE variations and the whole non-systematic variations approximately coincides, but in the negative range, it deviates greatly. Thus, the coupling of non-systematic variations in different regions is stronger under the condition of negative inlet flow angle.

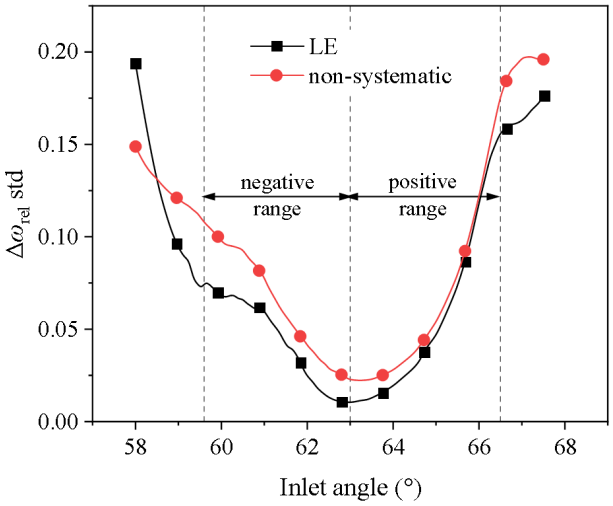

Figure 19. Comparison of the LE and the global non-systematic variations on $\Delta\omega_{rel}$ std.

5. Conclusions

A high accuracy blade manufacture variation decomposition method was proposed to decompose the manufacture variation to systematic variation and non-systematic variation. Thus, the statistical characteristics of the effect of manufacture variations on the blade aerodynamic performance can be quantified more clearly. The extraction of systematic variations is based on the reverse fitting of the measured blades by using blade design geometric parameters, while the extraction of non-systematic variation is the geometric variation between the measured blade and the systematic blades reconstructed.

The proposed manufacture variation decomposition method was applied to a set of 100 newly manufactured blades of a high-pressure compressor. The mean value and the standard deviation were used to analyze the statistical characteristics of the variations. Based on the results of the variation decomposition, the effects of different variation types on the blade performance and their coupling effect were analyzed. The following conclusions could be drawn:

(1) The proposed decomposition method could decompose the systematic variation into seven parameters used during blade geometry design process. Among them, the mean value of the inlet metal angle deviates from the design value obviously, and the relative deviations of the radii of the leading-edge and the trailing-edge have a great dispersion. This indicates that the manufacture variation caused a significant variation in the blade geometry, and even the inlet metal angle was systematically deflected. In addition, the distribution of all the systematic variations is close to the normal distribution.

(2) The non-systematic variation is the distance between the measured blade and the systematic blade obtained by parametric reconstruction using the systematic variation. That is, the non-systematic variation is a part of the manufacture variation after eliminating the systematic variation. The mean value of the non-systematic variation is close to zero. The standard deviation of the non-systematic variation accounts for

about 40% of the whole manufacture variation. This indicates that the systematic variation is the major component of the manufacture variation.

(3) The mean deviation of the measured blade ω_{rel} is mainly caused by systematic variation. The dispersion of $\Delta\omega_{rel}$ caused by non-systematic variation is obviously greater than that caused by systematic variation. In the positive range, the non-systematic variation determines the loss dispersion of the variation blades, while in the negative range, the loss dispersion is mainly caused by the systematic variations. In addition, the effects of systematic and non-systematic variations on $\Delta\omega_{rel}$ have a weak linear superposition effect, which requires further study and should be a caution for the related blade uncertainty quantification and robust design analyses.

(4) The systematic variations have a strong linear effect on the profile loss, and their coupling relationship can be modified by linear regression. Among the systematic variations, the profile loss is most sensitive to the inlet metal angle, and then followed by the radius of the leading-edge.

(5) The non-systematic variation in the leading-edge region has the most significant effect on the profile loss, which is much higher than that in other regions.

Author Contributions: Conceptualization, J.L. and X.Y.; methodology, J.L. and X.Y.; software, J.L.; validation, B.L. and G.A.; formal analysis, B.L., J.L., and X.Y.; investigation, B.L., J.L., X.Y., and G.A.; resources, B.L., X.Y., and G.A.; data curation, J.L. and X.Y.; writing—original draft preparation, J.L.; writing—review and editing, X.Y.; visualization, J.L. and X.Y.; supervision, B.L.; project administration, B.L. and G.A.; funding acquisition, B.L. All authors have read and agreed to the published version of the manuscript.

Funding: This research was funded by the National Natural Science Foundation of China (grant numbers: 51790511; 51806004) and National Science and Technology Major Project (Grant No. 2017-II-0001-0013).

Data Availability Statement: Not applicable.

Conflicts of Interest: The authors declare no conflict of interest.

References

1. Wong, C.Y.; Seshadri, P.; Scillitoe, A.; Duncan, A.B.; Parks, G. Blade Envelopes Part I: Concept and Methodology. *J. Turbomach.* **2022**, *144*, 061006. https://doi.org/10.1115/1.4053239.
2. Capiez-Lernout, E.; Soize, C.; Lombard, J.-P.; Dupont, C.; Seinturier, E. Blade Manufacturing Tolerances Definition for a Mistuned Industrial Bladed Disk. *J. Eng. Gas Turbines Power* **2005**, *127*, 621–628. https://doi.org/10.1115/1.1850497.
3. Wang, J.; Zheng, X. Review of Geometric Uncertainty Quantification in Gas Turbines. *J. Eng. Gas Turbines Power* **2020**, *142*, 070801. https://doi.org/10.1115/1.4047179.
4. Shi, W.; Chen, P.; Li, X.; Ren, J.; Jiang, H. Uncertainty Quantification of the Effects of Small Manufacturing Deviations on Film Cooling: A Fan-Shaped Hole. *Aerospace* **2019**, *6*, 46. https://doi.org/10.3390/aerospace6040046.
5. Vulpio, A.; Suman, A.; Casari, N.; Pinelli, M. Dust Ingestion in a Rotorcraft Engine Compressor: Experimental and Numerical Study of the Fouling Rate. *Aerospace* **2021**, *8*, 81. https://doi.org/10.3390/aerospace8030081.
6. Montomoli, F. *Uncertainty Quantification in Computational Fluid Dynamics and Aircraft Engines*, 2nd ed.; Springer: Cham, Switzerland, 2019; pp. 1–3.
7. Zhang, Q.; Xu, S.; Yu, X.; Liu, J.; Wang, D.; Huang, X. Nonlinear uncertainty quantification of the impact of geometric variability on compressor performance using an adjoint method. *Chin. J. Aeronaut.* **2022**, *35*, 17–21. https://doi.org/10.1016/j.cja.2021.06.007.
8. Garzon, V.E.; Darmofal, D.L. Impact of geometric variability on axial compressor performance. *J. Turbomach.-Trans. ASME* **2003**, *125*, 692–703. https://doi.org/10.1115/1.1622715.
9. Goodhand, M.N.; Miller, R.J. The Impact of Real Geometries on Three-Dimensional Separations in Compressors. *J. Turbomach.-Trans. ASME* **2012**, *134*, 021007. https://doi.org/10.1115/1.4002990.
10. Lange, A.; Voigt, M.; Vogeler, K.; Schrapp, H.; Johann, E.; Gummer, V. Impact of Manufacturing Variability on Multistage High-Pressure Compressor Performance. *J. Eng. Gas. Turbines Power-Trans. ASME* **2012**, *134*, 112601. https://doi.org/10.1115/1.4007167.
11. Lange, A.; Voigt, M.; Vogeler, K.; Schrapp, H.; Johann, E.; Gümmer, V. Impact of Manufacturing Variability and Nonaxisymmetry on High-Pressure Compressor Stage Performance. *J. Eng. Gas Turbines Power* **2012**, *134*, 032504. https://doi.org/10.1115/1.4004404.
12. Dow, E.A.; Wang, Q. Simultaneous robust design and tolerancing of compressor blades. In Proceedings of the ASME Turbo Expo 2014: Turbine Technical Conference and Exposition, Düsseldorf, Germany, 16–20 June 2014.

13. Kumar, A. Robust Design Methodologies: Application to Compressor Blades. Ph.D. Thesis, University of Southampton, Southampton, UK, 2006.
14. Kumar, A.; Keane, A.J.; Nair, P.B.; Shahpar, S. Robust design of compressor blades against manufacturing variations. In Proceedings of the ASME 2006 International Design Engineering Technical Conferences and Computers and Information in Engineering Conference, Philadelphia, PA, USA, 10–13 September 2006; pp. 1105–1118.
15. Luo, J.; Chen, Z.; Zheng, Y. A gradient-based method assisted by surrogate model for robust optimization of turbomachinery blades. *Chin. J. Aeronaut.* **2021**. https://doi.org/10.1016/j.cja.2021.07.019.
16. Wong, C.Y.; Seshadri, P.; Scillitoe, A.; Noel Ubald, B.; Duncan, A.B.; Parks, G. Blade Envelopes Part II: Multiple Objectives and Inverse Design. *J. Turbomach.* **2022**, *144*, 061007. https://doi.org/10.1115/1.4053240.
17. Goodhand, M.N.; Miller, R.J.; Lung, H.W. The Impact of Geometric Variation on Compressor Two-Dimensional Incidence Range. *J. Turbomach.* **2015**, *137*, 021007. https://doi.org/10.1115/1.4028355.
18. Lange, A.; Vogeler, K.; Gummer, V.; Schrapp, H.; Clemen, C. Introduction of a parameter based compressor blade model for considering measured geometry uncertainties in numerical simulation. In Proceedings of the 54th ASME Turbo Expo 2009, Orlando, FL, USA, 8–12 June 2009; pp. 1113–1123.
19. Lange, A.; Voigt, M.; Vogeler, K.; Schrapp, H.; Johann, E.; Gummer, V. Probabilistic CFD simulation of a high-pressure compressor stage taking manufacturing variability into account. In Proceedings of the ASME Turbo Expo 2010, Glasgow, Scotland, UK, 14–18 June 2010; pp. 617–628.
20. Garzon, V.; Darmofal, D. Using computational fluid dynamics in probabilistic engineering design. In Proceedings of the 15th AIAA Computational Fluid Dynamics Conference, Anaheim, CA, USA, 11–14 June 2001.
21. Garzon, V.E. Probabilistic Aerothermal Design of Compressor Airfoils. Ph.D. Thesis, Massachusetts Institute of Technology, MA, USA, 2003.
22. Schnell, R.; Lengyel-Kampmann, T.; Nicke, E. On the Impact of Geometric Variability on Fan Aerodynamic Performance, Unsteady Blade Row Interaction, and Its Mechanical Characteristics. *J. Turbomach.* **2014**, *136*, 091005. https://doi.org/10.1115/1.4027218.
23. Liu, J.; Yu, X.; Meng, D.; Shi, W.; Liu, B. State and effect of manufacture deviations of compressor blade in high-pressure compressor outlet stage. *Acta Aeronaut. Astronaut. Sin.* **2021**, *42*, 423796. https://doi.org/10.7527/S1000-6893.2020.23796.
24. Goodhand, M.N.; Miller, R.J. Compressor leading edge spikes: A new performance criterion. In Proceedings of the 54th ASME Turbo Expo 2009, Orlando, FL, USA, 8–12 June 2009; pp. 1553–1562.
25. Liu, B.; Liu, J.; Yu, X.; Meng, D.; Shi, W. Influence mechanisms of manufacture variations on supersonic/transonic blade aerodynamic performances. In Proceedings of the ASME Turbo Expo 2020: Turbomachinery Technical Conference and Exposition, Virtual, 21–25 September 2020.
26. Constantine, P.G.; Dow, E.; Wang, Q. Active Subspace Methods in Theory and Practice: Applications to Kriging Surfaces. *SIAM J. Sci. Comput.* **2014**, *36*, A1500–A1524. https://doi.org/10.1137/130916138.
27. Dow, E.A.; Wang, Q.Q. The Implications of Tolerance Optimization on Compressor Blade Design. *J. Turbomach.-Trans. ASME* **2015**, *137*, 101008. https://doi.org/10.1115/1.4030791.
28. Yu, X.; Li, M.; An, G.; Liu, B. A Coupled Effect Model of Two-Position Local Geometric Deviations on Subsonic Blade Aerodynamic Performance. *Appl. Sci.* **2020**, *10*, 8976. https://doi.org/10.3390/app10248976.
29. Kokoska, S.; Zwillinger, D. *CRC Standard Probability and Statistics Tables and Formulae*, 1st ed.; Chapman & Hall: Boca Raton, FL, USA; CRC Press: Boca Raton, FL, USA, 2000; pp. 341–343.
30. Reiss, R.D.; Thomas, M. *Statistical Analysis of Extreme Values: With Applications to Insurance, Finance, Hydrology and Other Fields*, 3rd ed.; Birkhäuser: Basel, Switzerland; Boston, MA, USA; Berlin, Germany, 2007; pp. 61–64.
31. Drela, M. A New Transformation and Integration Scheme for the Compressible Boundary Layer Equations, and Solution Behavior at Separation. Master's Thesis, Massachusetts Institute of Technology, Cambridge, MA, USA, 1983.
32. Drela, M. Two-Dimensional Transonic Aerodynamic Design and Analysis Using the Euler Equations. Ph.D. Thesis, Massachusetts Institute of Technology, Cambridge, MA, USA, 1986.
33. Küsters, B.; Schreiber, H.-A.; Köller, U.D.; Mönig, R. Development of advanced compressor airfoils for heavy-duty gas turbines: Part II—Experimental and theoretical analysis. In Proceedings of the ASME 1999 International Gas Turbine and Aeroengine Congress and Exhibition, Indianapolis, IN, USA, 7–10 June 1999.
34. Liu, B.; Xu, X.; Yu, X.; Zhu, H. Experimental and numerical investigation on the flow near the leading-edge of controlled diffusion airfoil. *J. Eng. Thermophys.* **2019**, *40*, 1767–1774.
35. Ross, S.M. *Introduction to Probability and Statistics for Engineers and Scientists*; Elsevier Academic Press: Burlington, NJ, USA, 1972; Volume 9, pp. 353–439.